20th ASM Heat Treating Society Conference Proceedings, 9-12 October 2000, St. Louis, MO, ASM International, 2000

Microstructure and Fatigue Resistance of Carburized Steels

J.P. Wise, G. Krauss, D.K. Matlock
Colorado School of Mines, Golden, Colorado

Abstract

A summary is presented of recent research on the microstructure and bending fatigue performance of several carburizing steels. Two fatigue optimization approaches were explored: alloy chemistry and processing. Compositions were varied with respect to sulfur, phosphorous, manganese, and silicon. In each case, maximum composition limits of the elements were identified that resulted in decreases in the presence of fatigue crack initiators. The suppression of manganese sulfides, intergranular cementite, and intergranular oxides substantially increased bending fatigue endurance limits. A carburizing process study showed that reductions in case carbon content, through low carburizing potentials and reheat treatments, resulted in less retained austenite, larger surface residual stresses, and consequently, higher endurance limits. Shot peening created the most dramatic increases in fatigue performance, due to the generation of very large residual stresses. The entire set of data summarized in this report was statistically analyzed to reveal broad trends in bending fatigue research. Prior austenite grain size in the case and surface residual stresses had the largest effects on bending fatigue endurance limit. Case grain refinement was most effectively achieved through reheat treatments, while shot peening was the primary means to significantly increase compressive residual stresses in the specimen surface.

Introduction

Steel gears fail in bending fatigue at nominal stresses well below the bulk yield strength of the material due to the presence of microstructural features that locally raise the applied stress. Maximum gear performance is achieved when the metallurgist understands how microstructures respond to applied stress and how to control, or compensate for, these microstructures through alloy and process design. Carburizing improves gear performance by enhancing surface properties. The addition of carbon into the surface of a component creates a composite material consisting of a high-carbon steel case and a low-carbon steel core. When this steel composite is quenched to martensite and tempered, the high hardness and strength of the case microstructure, combined with the favorable case compressive residual stresses developed during quenching, produce a high resistance to fatigue.

This work identifies the important chemistry, processing, and microstructural variables that govern the bending fatigue performance of carburized steels. The discussion concentrates on recent bending fatigue research and is divided into two sections: effects of alloy chemistry and effects of processing techniques. All fatigue research was performed with a constant specimen geometry, offering the unique opportunity to perform a statistical analysis to extract broad trends in bending fatigue behavior.

Fatigue Research

Testing. The studies cited throughout this work were part of a large effort to assess the role of alloy chemistry, heat treatment, and shot peening on the microstructure and bending fatigue performance of several carburizing steels. All testing was done with the cantilever beam bending fatigue specimen shown in Figure 1. The specimen incorporates a 3.2-mm radius designed to simulate a single gear tooth. Bending fatigue testing was performed on commercial test frames. Specimens were cyclically loaded by a combination of a rotating weight and a static load imposed by a constant displacement. Tests were run at a frequency of 30 Hz with a ratio of minimum to maximum stress of 0.1. Keeping specimens in tension at all times preserved fracture surfaces for later examination. S-N curves for each experimental condition were created using approximately 40 specimens. Three tests were performed at each stress level, and endurance limits were defined as the maximum stress that produced three consecutive run-outs at ten million cycles.

Several specimen characteristics were kept constant to isolate the effects of alloy chemistry and processing approaches on fatigue performance. Following machining, the specimens were chemically polished to create a uniform surface finish prior to carburizing. All specimens were carburized to a nominal case depth of 1 mm to 50 HRC, which resulted in constant residual stresses near 100 MPa in compression at the specimen surface.

The relatively low residual stresses were a result of the type of specimen used. The small specimens were easily through-hardened upon quenching. Consequently, much lower residual stresses were generated in the test specimens as compared to those achieved in actual gears.

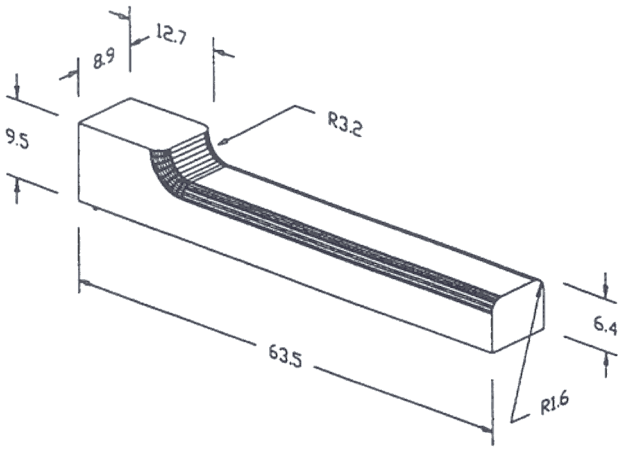

Figure 1. Cantilever beam bending fatigue specimen. Measurements are in millimeters.

Specimen Failure Mechanisms. The fatigue performance of the steels reviewed in this work was closely related to the mechanism by which the initial fatigue crack formed. In direct-quenched gear steels with moderate to good endurance limits of 1000-1300 MPa, the initial fatigue crack predominantly formed as a result of the separation of prior austenite grain boundaries at the component surface[1]. This intergranular fracture is related to phosphorous segregation to, and cementite formation on, austenite grain boundaries[2]. Intergranular initiation sites were composed of a single grain boundary or often extended several grains into the interior of the component. High endurance limits, above 1400 MPa, were usually associated with transgranular crack nucleation within the prior austenite grains[3]. Prior austenite grain sizes controlled the mode of crack initiation, as initiation modes have been successfully altered from intergranular to transgranular by refining the austenite grain size through reheat treatments after carburizing[4]. Figure 2 shows a typical fracture path of a bending fatigue specimen failure. The crack in the figure begins with a small region of grain boundary separation. This intergranular crack forms as soon as an initial stress is placed on the specimen[5]. The sharp tip of the intergranular crack then becomes the starting point for stable transgranular fatigue crack growth. When the transgranular crack reaches a critical size, it becomes unstable and final overload fracture of the specimen begins.

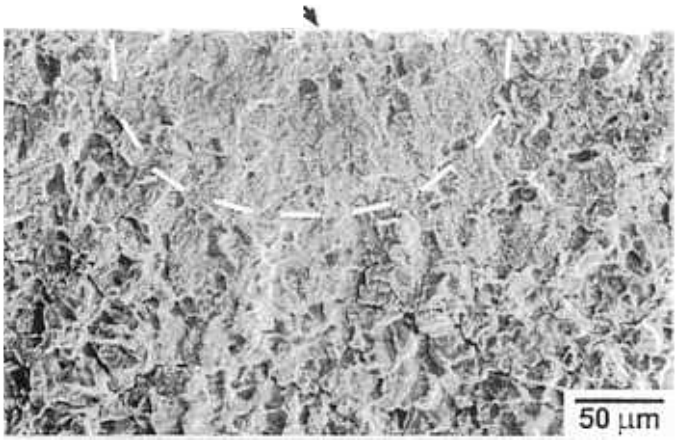

Figure 2. Overview of fatigue fracture in a carburized SAE 4320 steel, showing elliptical transgranular crack centered on an intergranular initiation site marked by arrow. SEM micrograph.

Design of Alloy Chemistry

While guidelines for alloy chemistry for optimum fatigue resistance are continually being refined, some desirable characteristics are generally agreed upon. The case should consist of a high-carbon tempered martensite with some retained austenite. Ni, Cr, Mn, and Mo increase a steel's hardenability and prevent the formation of non-martensitic transformation products upon quenching. In addition, Ni is often added to improve martensite toughness. Large carbides, oxides, and other second-phase particles are to be avoided. These structures may either combine with other features that initiate fatigue cracks, or in the absence of such features, serve as the sole source of fatigue crack initiation. Consequently, S, P, and strong oxide-formers (Cr, Si, Mn) must be carefully controlled. Finally, small prior austenite grains sizes are beneficial to fatigue resistance, as discussed previously. Fine carbides, nitrides, and carbonitrides of Al, V, Nb, and Ti pin grain boundaries at carburizing temperatures.

The following is a review of recent research on alloy chemistry effects on the microstructure and fatigue performance of carburized steels. In each case, an element, or combination of elements, formed an undesirable second-phase that contributed to fatigue crack initiation by weakening of prior austenite grain boundaries. The goal of these works was to identify critical levels of the elements to avoid significant loss in fatigue resistance.

Sulfur: The Effect of Non-Metallic Inclusions. Sulfur exists in steel primarily in the form of manganese sulfide inclusions. While MnS particles greatly improve machinability, they act as stress concentrators to facilitate fatigue crack nucleation. The effects of MnS on fatigue performance were demonstrated by a study that systematically varied sulfur content in an SAE 8219-type steel[1]. The amount of manganese sulfide inclusions present in the microstructure was found to be proportional to the bulk sulfur content. As the number of sulfides

increased, they became more likely to be associated with fatigue crack initiation sites in bending fatigue tests. In all alloys, the initial fatigue crack consisted of a cluster of separated grain boundaries at the specimen surface. The MnS inclusions, however, apparently provided an extra source of stress concentration to facilitate fatigue crack nucleation, as shown in Figure 3. Figure 4 shows how the increase in bulk sulfur content from 0.006 to 0.029 weight percent resulted in a drop in the endurance limit from 1260 to 1070 MPa. Consequently, a gear steel designer must weigh this lowered fatigue performance against gains in machinability associated with higher sulfur levels.

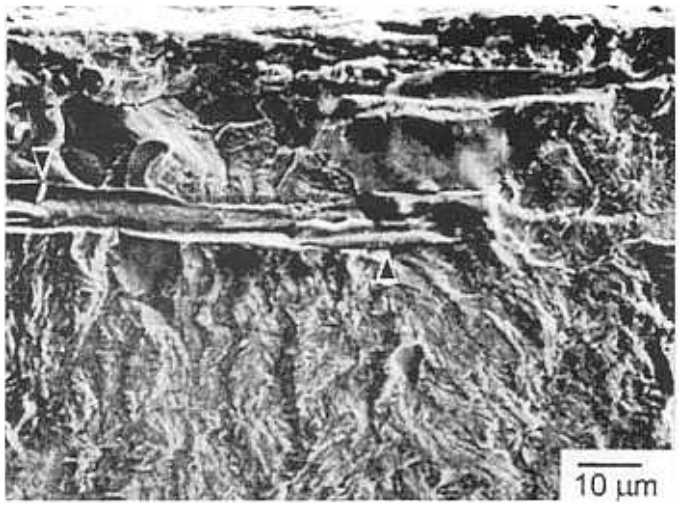

Figure 3. Manganese sulfide inclusions at the fatigue initiation site in a carburized SAE 8219-type steel. SEM micrograph.

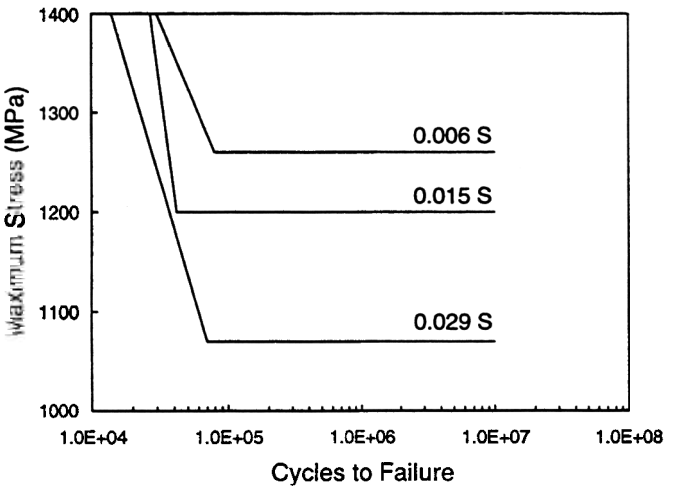

Figure 4. Effect of sulfur content on the S-N curve of a carburized SAE 8219-type steel. Concentrations are expressed in weight percent.

Phosphorous: Grain Boundary Cementite Formation. In medium carbon steels, tempering is required to cause intergranular fracture. For example, tempered martensite embrittlement (TME) and temper embrittlement (TE) develop after heating between 260-370°C and 375-575°C respectively[6,7]. However, in steels containing more than 0.5 weight percent carbon, susceptibility to intergranular embrittlement occurs immediately after quenching and persists after tempering at temperatures below those at which TME develops. This phenomenon, termed quench embrittlement, is characterized by cementite formation on austenite grain boundaries during austenitizing and/or quenching[2].

Phosphorous strongly promotes quench embrittlement by its segregation to austenite grain boundaries and its stabilizing effect on cementite. A study on the effects of phosphorous content in a carburized SAE 4320 steel showed that high phosphorous levels enhance phosphorous segregation to austenite grain boundaries and considerably lower bending fatigue endurance limits[2]. As shown in Figure 5, when bulk phosphorous content exceeded 0.017 weight percent, endurance limit dropped significantly. An increase in phosphorous from 0.017 to 0.031 weight percent reduced endurance limits from 1075 to 875 MPa. Despite the beneficial effects of low phosphorous levels on endurance limits, fatigue crack initiation was still characterized by intergranular cracking in all direct-quenched alloys.

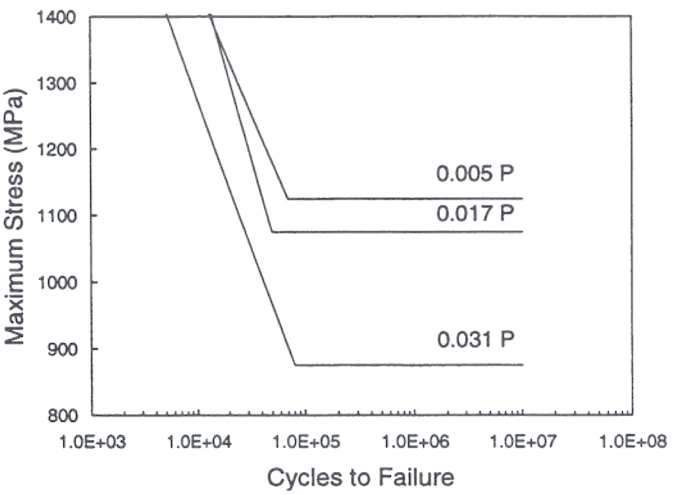

Figure 5. Effect of phosphorous content on the S-N curve of carburized 4320 steel. Concentrations are expressed in weight percent.

Manganese and Silicon: Intergranular Oxidation. The atmosphere within a gas carburizing furnace is composed primarily of CO, CO_2, H_2, H_2O, and N_2. Carbon potential is controlled by the addition of a hydrocarbon gas such as methane or propane. In addition to these gases, a small amount of oxygen is inevitably present, causing surface oxidation during carburizing. Silicon, manganese, and chromium commonly form oxides when exposed to a gas carburizing atmosphere. Oxides typically form on austenite grain boundaries to a depth of 10 to 20 μm, due to the

ease of oxygen diffusion along these paths. Similar to the MnS inclusions discussed previously, oxides can facilitate nucleation of fatigue cracks. In addition, surface oxidation removes elements such as chromium and manganese that provide hardenability to the matrix. This may result in the formation of non-martensitic microstructures such as ferrite, bainite, or pearlite upon quenching[8]. The formation of the non-martensitic structures compromises both strength and compressive residual stresses.

A study of the effects of high oxide-potential elements in a gas carburized SAE 4320-type steel has shown that control of alloy chemistry can virtually eliminate intergranular oxidation (IGO) and subsequently increase fatigue performance[9]. In a low-Cr modified 4320 steel, silicon levels were systematically reduced from 0.34 to 0.07 weight percent, resulting in the corresponding reduction in the IGO depth as seen in Figure 6. With the decrease in stress concentration associated with the oxides, bending fatigue endurance limits improved from approximately 1100 to 1500 MPa, as shown in Figure 7. Using the low-Si alloy (0.07 Si) as a base, manganese contents were subsequently reduced from 0.65 to 0.31 weight percent in an attempt to further improve oxidation and fatigue properties. The depth of oxidation did not appreciably decrease with lower Mn levels; however, endurance limits improved from 1250 to 1350 MPa with the Mn reduction. The low-Mn alloy had very limited oxide coverage on the near surface grain boundaries. Thus, both oxide depth as well as the extent of grain boundary coverage seem to impact the ease of fatigue crack initiation at prior austenite grain boundaries. Figure 8 depicts the intergranular fracture origin of a high-Mn high-Si alloy, showing patterns on the fatigue initiation site indicative of oxide formation.

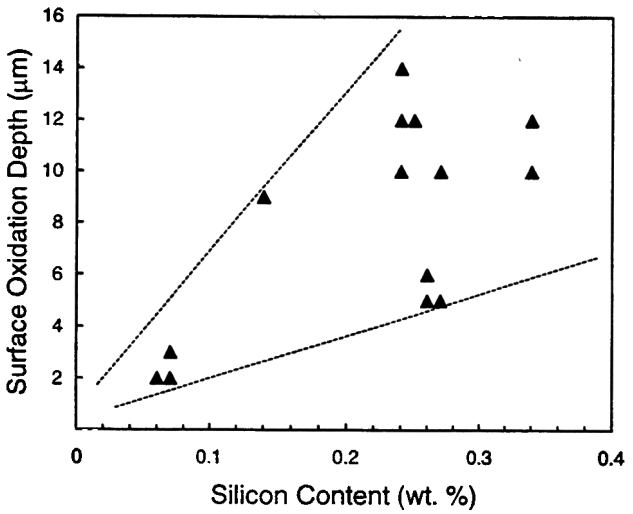

Figure 6. Effect of silicon content on oxidation depth in a carburized modified 4320 steel.

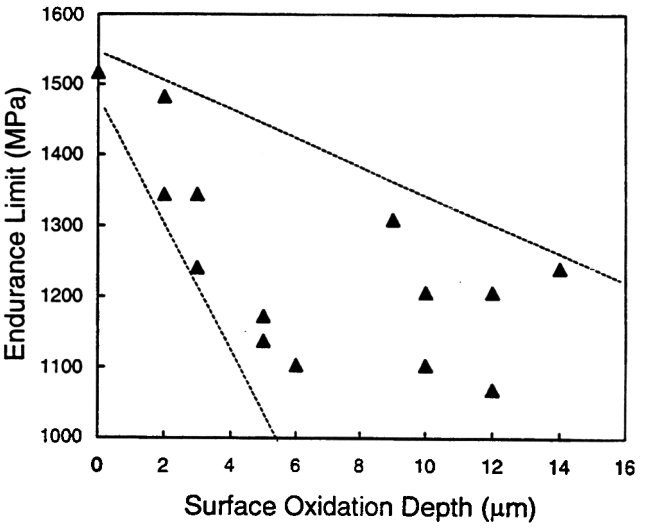

Figure 7. Influence of intergranular oxidation depth on the bending fatigue endurance limit of a carburized modified 4320 steel.

Figure 8. Oxide coverage on the intergranular fracture origin of a 0.6Mn-0.14Si modified 4320 Steel. SEM micrograph.

Intergranular oxidation has also been successfully controlled through processing techniques; however, a reduction in surface oxidation does not always translate into improved fatigue performance. Unlike conventional gas carburizing, plasma and vacuum carburizing are performed in atmospheres that do not contain oxygen, and the degree of IGO is very small. In addition, these processes can achieve higher carburizing temperatures and carbon potentials, significantly reducing carburizing time. However, excessive austenite grain growth and difficult carbon potential control is often associated with these techniques, leading to reduced fatigue performance.

Process Design: Carburizing and Shot Peening

Carburizing introduces a gradient in the surface microstructure and mechanical properties. The hardness and strength of martensite increase with increasing carbon content. Therefore, the highest hardness of a hardened carburized steel is at or close to the surface, typically in the range of 58-62 HRC. Hardness may peak at a distance from the surface if large amounts of retained austenite, which is much softer than martensite, offset the high hardness of the martensite immediately adjacent to the surface where the carbon content is at its highest. Increasing carbon content significantly lowers M_S temperatures and depresses the entire temperature range for martensitic transformation to below room temperature. Consequently, there are almost always significant amounts of retained austenite in the cases of carburized steels quenched to room temperature. Retained austenite plays a large role in the fatigue of carburized steels, and amounts on the order of 20 to 30 volume percent are common in the near-surface cases of direct-quenched gears. At the high strain amplitudes present in low-cycle fatigue, retained austenite undergoes deformation-assisted transformation to martensite, extending fatigue life[10]. Conversely, retained austenite may be detrimental in high-cycle fatigue, for the retention of austenite reduces hardness and compressive residual stresses, facilitating fatigue crack initiation.

Two heat treatment approaches were considered in the research reviewed below: direct quenching and reheating. Direct quenching is the most common carburizing treatment. The component is typically quenched in oil from the carburizing temperature and is then tempered to achieve the final properties. Reheat treatments add an additional step to the direct-quenched method. After quenching from the carburizing temperature, the component is intercritically austenitized before a final quench. Carbide particles precipitate during the intercritical treatment, reducing the matrix carbon content.

Shot peening mechanically strengthens the surface of a carburized steel component through work hardening and the transformation of retained austenite to martensite. Furthermore, the cold work and martensitic transformation induce large compressive residual stresses. Shot peening may also affect surface roughness. The impact of the steel shot often smooths coarse machining marks, reducing stress concentrations that may play a role in fatigue crack initiation.

Carburizing: Carbon Potential and Reheat Treatments. As discussed earlier, strength gains realized through carburizing increase with carbon potential, yet excessive carbon results in incomplete martensitic transformation upon quenching. Large amounts of retained austenite diminish compressive residual stresses and lower yield strengths, resulting in a decrease in high-cycle fatigue performance. Furthermore, high-carbon steels are especially prone to quench embrittlement. Consequently, optimum bending fatigue performance depends on selecting the carbon potential that maximizes case strength without compromising residual stress and resistance to embrittlement.

An investigation was performed to study the response of a carburized SAE 4320 steel to carbon potentials of 0.6, 0.85, 1.05, and 1.25 weight percent[11]. Effects on retained austenite content, residual stress state, and bending fatigue endurance limits were assessed. A reheat step after carburizing was added to the processing of some specimens to refine austenite grain size and to lower the solute carbon content in the case through the formation of carbides. Figures 9-a and 9-b show how increased carbon resulted in higher retained austenite contents and lower residual stresses at the specimen surface. Consequently, bending fatigue endurance limits were found to decrease with increasing carbon as shown in Figure 9-c. The plots also show that the reheat treatments successfully reduced the solute carbon in the case, contributing to the observed improvements in retained austenite, residual stress, and endurance limit over conventionally treated steels.

Shot Peening. Shot peening was evaluated with the use of soft steel shot, hard steel shot, and a two-step (hard shot + low intensity-small shot) peening treatment on a carburized SAE 4320 steel[12]. All peening processes significantly reduced retained austenite at the specimen surface, from 28 volume percent in the as-carburized condition to less than 9 volume percent after all peening treatments. Surface hardness increased from 57 to 61 HRC, and compressive surface residual stresses dramatically increased from 100 to almost 1000 MPa. As a result, bending fatigue endurance limits increased from 1070 to over 1400 MPa for all peening treatments, as shown in Figure 10.

Additional shot peening studies were performed on carburized SAE 4023, 4320, and 9310 steels[13]. Similar to the results discussed above, compressive residual stresses at the specimen surface increased from 100 to as high as 1450 MPa after peening. Shot peened alloys consistently achieved endurance limits near 1500 MPa, approximately 250-350 MPa higher than in typical unpeened specimens.

Statistical Analysis of Specimen Characteristics and Their Effect on Bending Fatigue Performance

The myriad of variables that can affect bending fatigue behavior make it very difficult to determine exactly what should be the focus of research programs devoted to increasing performance. The studies presented above offered a unique opportunity to apply statistical methods to a large set of data in an effort to extract significant trends to aid in chemistry and process design. In each research program summarized above, a broad spectrum of specimen characteristics was recorded: retained austenite content, prior austenite grain size of the case and core, extent of intergranular oxidation, surface roughness in the specimen root, and the case profiles of residual stress, hardness, and carbon content. The analysis below begins with correlation coefficient calculations to determine those variables that show the strongest association to endurance limit. Using multiple regression techniques, these variables are then considered in the construction of a quantitative model to predict fatigue performance.

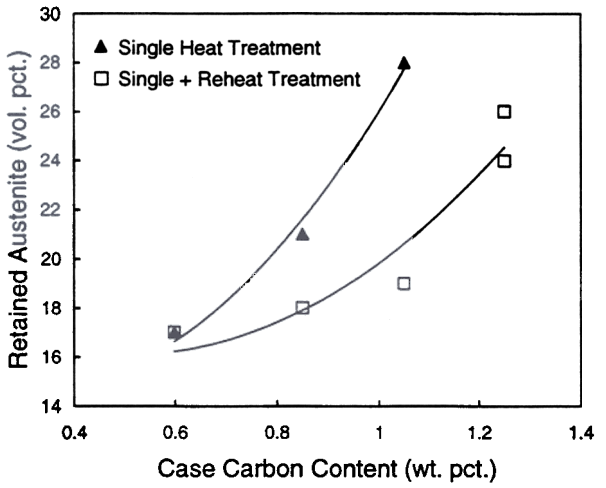

(a)

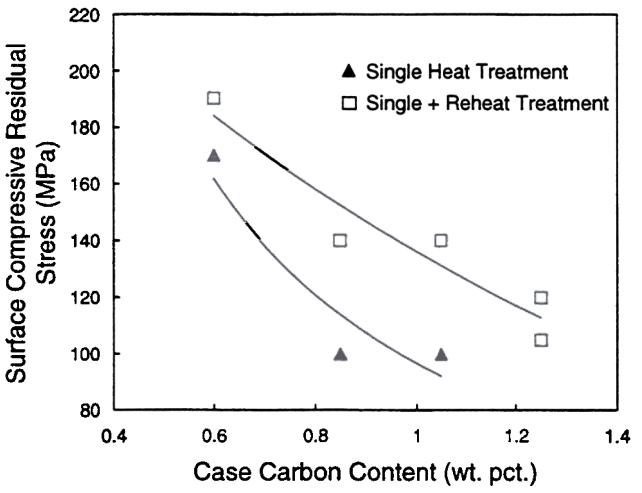

(b)

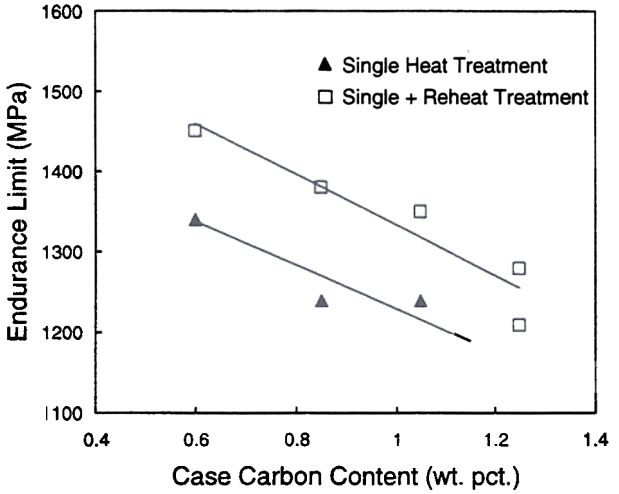

(c)

Figure 9. The effect of carbon potential on (a) retained austenite, (b) surface residual stress, and (c) the bending fatigue endurance limit of a carburized SAE 4320 steel.

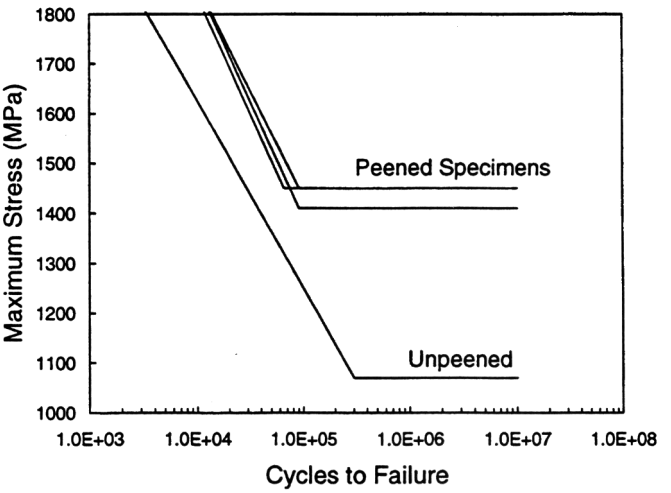

Figure 10. Effect of shot peening on the S-N curve of a carburized SAE 4320 steel.

Correlations Between Endurance Limit and Specimen Characteristics. The correlation coefficient, r, provides a guide as to which variables have the most pronounced effect on the variable of interest - in this case endurance limit. Specifically, the correlation coefficient is a measure of the strength of the linear relationship between two variables. When a linear relationship is nonexistent, the r-value is close to zero. A perfectly linear dependence results in an r-value of 1 or –1, depending on whether a positive or negative linear relationship exists between the two variables.

Several variables were considered to determine those with the strongest correlations with bending fatigue endurance limit: surface carbon content, surface hardness, case depth to 50 HRC, residual stress, retained austenite, case and core grain size, depth of intergranular oxidation, and surface roughness in the specimen root along the longitudinal axis of the specimen. Residual stress and retained austenite profiles into the case exist for many data sets; thus values from the surface as well as from deeper into the case were considered. Figure 11 displays the absolute value of the correlation coefficient of each variable with endurance limit. Absolute values were used so the strengths of the relationships could be easily compared. The plot shows that surface residual stress and prior austenite grain size in the case exhibit the strongest relationships with endurance limit.

In the statistical design of an experiment to measure the impact of a variable, one would select values for that variable that would span an appreciable range to insure the variable was effectively tested. In the present study, however, the analysis was performed within the confines of test conditions having been already established. This non-ideal experiment setup was monitored to insure false conclusions were not drawn. For example, intergranular oxidation data do not vary significantly. Almost all of the surface oxides were found to be about 10 μm deep, and thus the oxidation correlation results should not be applied to a wide range of depths. Conversely, case grain size varied to a large degree, from 4 μm to 18 μm, across the total data set. Specimen characteristics that varied little include oxidation

depth, retained austenite, the surface roughness parameters, and to a certain extent residual stress.

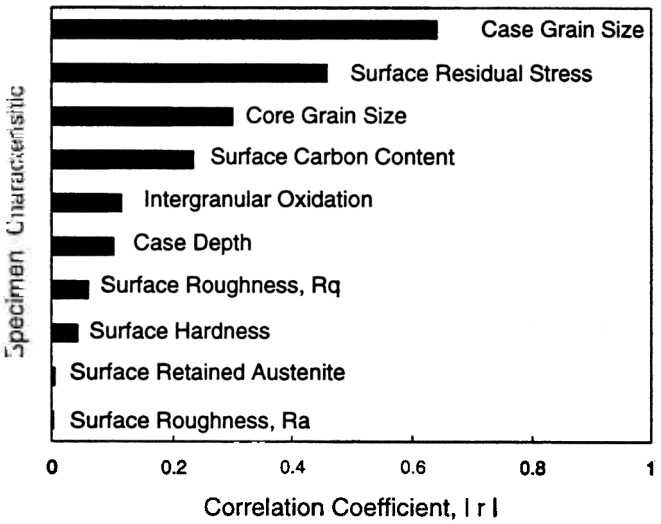

Figure 11. Correlations of measured specimen characteristics to bending fatigue endurance limit.

Multiple Regression Model for Endurance Limit. A multiple regression analysis was used to describe the bending fatigue endurance limit by an equation of the general form:

$$Endurance\ Limit = \beta_0 + \beta_1 v_1 + \beta_2 v_2 + \beta_3 v_3 + ... \qquad (1)$$

where the coefficients are constants and v_i, i=1,2,3.., represent the independent variables. Three statistical measurements were used to choose the combination of variables for the model: the multiple coefficient of error (R^2), the F-statistic, and the P-value. R^2 is a measure of how well a model fits a set of data. The F-statistic is a test of the hypothesis that at least one of the regression coefficients in Eq. 1 is not zero, or is a determination of whether the model is more useful than no model at all. The P-value is derived from the two-tailed t-distribution. It is the probability that a regression coefficient can be considered statistically equivalent to zero. In summary, the goal of the regression analysis is to create a model that maximizes the R^2 and F-statistic while minimizing the P-values for the independent variables.

A regression model to describe bending fatigue endurance limit was created by starting with a very complex equation containing all the specimen characteristics and subsequently simplifying the model by eliminating variables with large P-values. With the reduction in number of variables, the fit to the experimental data was less accurate, yet overall confidence in the regression coefficients increased. The most appropriate model seems to be one that contains only the effects of case grain size and surface residual stress. The details of the model are shown in Eq. 2 and Table 1. While all functional relationships between endurance limit and grain size produced equally good results, a Hall-Petch type dependence on grain size was chosen because of its significance in materials strengthening. The negative sign on the residual stress coefficient is due to the convention used in this work that defines compressive stresses as negative.

Figure 12 is a graphical representation of the regression model detailed in Table 1. The figure is a contour plot showing lines of constant endurance limit as a function of case grain diameter and surface residual stress. Moving from the top-right to the bottom-left of the plot, case grains become finer and residual stresses more compressive, yielding higher endurance limits. The multiple regression equation is only valid over the range in which the variables were tested. Consequently, the plot should only be referenced for case grain diameters between 4 and 18 μm and residual stresses between approximately 0 and 1500 MPa in compression. Within this region, the standard error of the model is 121 MPa. Figure 13 compares the experimental data to values predicted by the model.

$$\text{Endurance Limit (MPa)} = 750 + 1352 \times (\text{Case Grain Diam.}\ (\mu m))^{-\frac{1}{2}} - 0.19 \times (\text{Surface Residual Stress (MPa)}) \qquad (2)$$

Table 1: Multiple Regression Model Predicting Bending Fatigue Endurance Limit

R^2	0.551	
F-statistic	36.8	
Variable	Regression Coefficient	P-value
Y-Intercept	750.1	
(Case Grain Diameter)$^{-1/2}$, μm	1352	1.82×10^{-8}
Surface Residual Stress, MPa	-0.1887	3.20×10^{-6}

Determiners of Grain Size and Residual Stress. In an effort to guide the design of alloys to achieve fine grains and highly compressive residual stresses, correlation calculations were performed to determine which specimen characteristics most strongly affect the two variables of interest. It was necessary to omit shot peened alloys from the calculations to obtain meaningful residual stress correlations. Shot peening creates high compressive residual stresses that exaggerate the effects of other variables that may have just happened to have extreme values in shot peened studies. Case grain size correlations encompass all data, including shot peened alloys. Figure 14 shows the results of the correlation calculations, limited to the variables that had the strongest correlations. Significant correlations to case grain size are shared with core grain size and several alloying additions. Residual stress correlations show the effects of several elements as well as surface hardness, core grain size, and case depth.

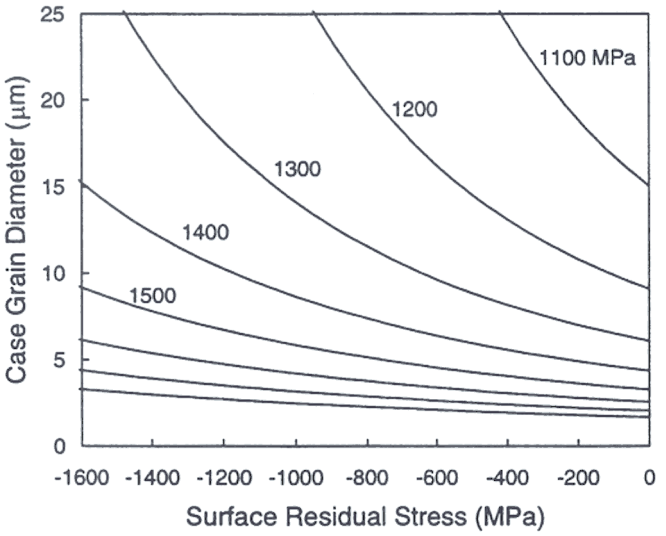

Figure 12. Graphical representation of regression model in Table 1 depicting constant endurance limit contours as a function of case grain size and surface residual stress.

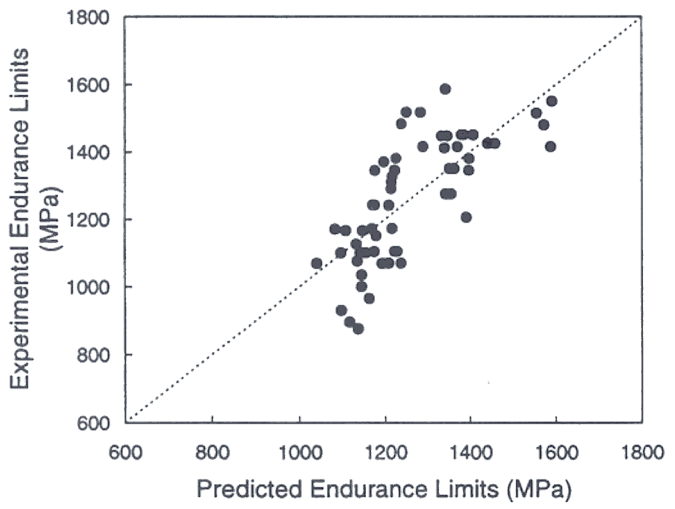

Figure 13. Comparison between experimental endurance limits and model predictions.

The case grain size correlations show some interesting relationships. The high correlation with core grain size is expected, because those factors that promote a fine case grain size usually affect the core similarly. A cause and effect relationship between case and core grain size is most likely not present. The second strongest correlation to case grain size is aluminum content. In light of the grain refining nature of aluminum nitride, the correlation is expected. Nitrogen does not show a strong correlation to case grain size; however, nitrogen levels were fairly consistent across the research projects and thus would not be expected to show significant correlations. The lack of any strong relationships to case grain size reflects the dependence of grain size on variables other than microstructure and chemistry. Many reheat treatments that produce fine grain sizes were part of this study, and they can easily overshadow the effects of other variables. The carbon potential study reviewed previously found that case grain sizes were reduced nearly in half from a diameter of 9.4 μm to 4.8 μm when a reheat step was added.

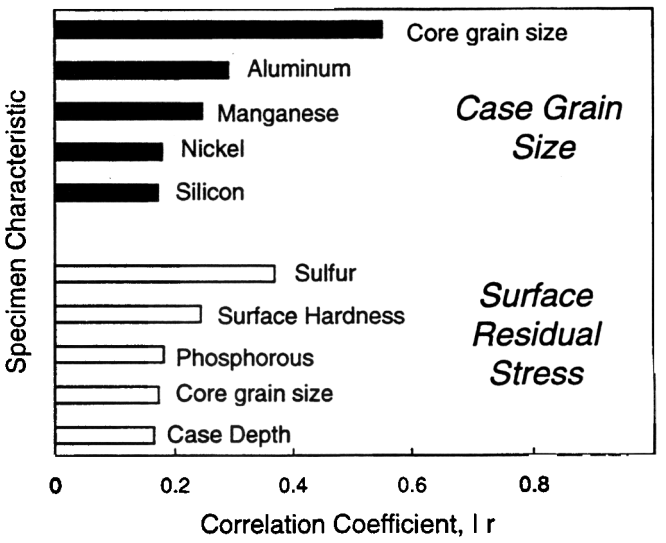

Figure 14. Correlation of specimen characteristics to case grain size and surface residual stress.

The residual stress calculations revealed a few relationships that may be significant. The levels of sulfur and phosphorous are most likely not determiners of residual stress despite the relatively high correlation coefficients for these elements. The surface hardness relationship may be indicative of a more complete martensitic transformation upon quenching, which would be expected to influence the residual stress state. The depth of the carburized case, also, would be expected to impact the stress state at the surface. Like grain size, residual stress was found to depend primarily on processing, not chemistry or microstructural characteristics. In all cases, shot peening dramatically increased compressive residual stresses from values of 100 MPa in unpeened specimens to 1100-1500 MPa after peening.

Perspectives on the Statistical Analysis. The statistical analysis consolidated data taken over a decade of work by several researchers on many different alloy compositions. Despite the many sources of variation inherent with this experimental setup, a few very significant determiners of bending fatigue endurance limit emerged: case grain size and surface residual stress. A few factors that are known to affect fatigue performance were not exposed in the broad study of the fatigue data. For example, the detrimental effects of the impurity elements, sulfur and phosphorous, discussed earlier were not revealed in this analysis. Both bulk S and P varied little in the total data set. Similarly, the statistical analysis did not reveal retained austenite as a significant

factor in fatigue, although an austenite effect is well known. The relatively constant carburizing conditions used throughout the studies confined retained austenite contents to a narrow range, between approximately 20 and 25 volume percent. This lack of variation prevented an accurate assessment of the impact of retained austenite.

Conclusions

The following conclusions are based upon data taken over a decade of work by several researchers on many different alloy compositions. It has been shown that significant gains in the fatigue performance of gas-carburized gear steels can be realized through proper control of alloy chemistry and processing. Significant results are as follows:

1. Elevated sulfur levels produced a high density of MnS inclusions. The MnS inclusions act as stress concentrators that facilitate fatigue crack initiation. As bulk sulfur content in a carburized SAE 8219-type steel increased from 0.006 to 0.029 weight percent, the endurance limit dropped from 1260 to 1070 MPa.

2. Phosphorous strongly promotes intergranular fatigue crack initiation through its stabilizing effect on cementite. When phosphorous levels exceeded 0.017 weight percent in a carburized SAE 4320 steel, the endurance limit dropped sharply. An increase in P from 0.017 to 0.031 weight percent reduced endurance limits from 1075 to 875 MPa.

3. Intergranular oxidation, associated with gas carburizing, was effectively controlled by reducing the levels of high oxide-potential elements. Reductions in silicon in a low-Cr SAE 4320 steel resulted in smaller oxide depths and higher endurance limits. Reductions in manganese improved fatigue performance of the low-Si alloy to a lesser degree, primarily by reducing the extent of oxide coverage on austenite grain boundaries.

4. Reductions in case carbon content, through lower gas carburizing potentials and the use of reheat treatments, resulted in less retained austenite and higher compressive residual stresses, leading to improvements in the endurance limit of a carburized SAE 4320 steel.

5. Shot peening significantly enhanced compressive surface residual stresses from 100 MPa to over 1000 MPa in several carburizing steel grades. As a result, bending fatigue endurance limits of 1400 to 1500 MPa were achieved, 250-380 MPa higher than those of unpeened specimens.

6. A statistical analysis of the entire set of bending fatigue data identified prior austenite grain size in the case and surface residual stress as the most important factors that determine endurance limit. A multiple regression model to predict endurance limit achieved an R^2 value of 0.56. Case grain refinement was most effectively achieved through reheat treatments, while shot peening was found to be the primary means to significantly increase compressive surface residual stresses.

Acknowledgements

This project, and the research reviewed in this work, was supported by the Advanced Steel Processing and Products Research Center, an industry/university cooperative research center at the Colorado School of Mines in Golden, CO. The authors would like to acknowledge all the researchers that contributed to the work presented here: J.L. Pacheco, K.A. Erven, R.E. Cohen, J.A. Sanders, D.J. Medlin, R.S. Hyde, J. Kristan, and B.E. Cornelissen.

References

[1] K.A. Erven, D.K. Matlock, and G. Krauss, "Effect of Sulfur on Bending Fatigue of Carburized Steel", Journal of Heat Treating, vol. 9, no. 1, 1991, pp. 27-35.

[2] R.S. Hyde, D.K. Matlock, and G. Krauss, "Quench Embrittlement: Intergranular Fracture Due to Cementite and Phosphorous in Quenched Carbon and Alloy Steels", Proceedings of the 40th Mechanical Working and Steel Processing Conference, pp. 921-928.

[3] J.L. Pacheco and G. Krauss, "Microstructure and High Bending Fatigue Strength in Carburized Steel," Journal of Heat Treating, vol. 7, no. 2, 1989, pp. 77-86.

[4] R.S. Hyde, G. Krauss, and D.K. Matlock, "The Effect of Reheat Treatments on Fatigue and Fracture of Carburized Steels," SAE Report No. 940788, Society of Automotive Engineers, Warrendale, PA, 1994.

[5] R.S. Hyde, R.E. Cohen, D.K. Matlock, and G. Krauss, "Bending Fatigue Crack Characterization and Fracture Toughness of Gas Carburized SAE 4320 Steel," SAE Report No. 920534, Society of Automotive Engineers, Warrendale, PA, 1992.

[6] N. Bandyopadhyay and C.J. McMahon, Jr., "The Mico-Mechanisms of Tempered Martensite Embrittlement in 4340-Type Steels", Metallurgical Transactions A, Vol. 14A, 1983, pp. 1313-1325.

[7] M. Gutmann, P. Dumoulin, and M. Wayman, "The Thermodynamics of Interactive Co-segregation of Phosphorous and Alloying Elements in Iron and Temper-Brittle Steels", Metallurgical Transactions A, Vol. 13A, 1982, pp. 1693-1711.

[8] W.E. Dowling Jr., W.T. Donlon, W.B. Coppel, R.A. Chernenkoff, and C.V. Darragh, "Bending Fatigue Behavior of Carburized Gear Steels: Four-Point Bend Test Development and Evaluation", SAE Report No. 960977, Society of Automotive Engineers Inc., Warrendale, Pa., 1996.

[9] B.E. Cornelissen, "Alloying and Processing Approaches to Improved Bending Fatigue Performance of Carburized Gear Steels", Ph.D. Thesis, Colorado School of Mines, Golden, Colorado, June, 1999.

[10] M.A. Zaccone, J.B. Kelly, and G. Krauss, "Stain Hardening and Fatigue of Simulated Case Microstructures in Carburized Steel," Carburizing: Processing and Performance, ASM International, Lakewood, Colorado, July 12-14, 1989, pp. 249-265.

[11] D.J. Medlin, B.E. Cornelissen, D.K. Matlock, G. Krauss, and R.J. Filar, "Effect of Thermal Treatments and Carbon Potential on Bending Fatigue Performance of SAE 4320 Gear Steel", SAE Report No. 1999-01-0603, Society of Automotive Engineers Inc., Warrendale, Pa., 1999.

[12] J.A. Sanders, "The Effects of Shot Peening on the Bending Fatigue Behavior of a Carburized SAE 4320 Steel", M.S. Thesis, Colorado School of Mines, Golden, Colorado, August, 1993.

[13] D.J. Medlin, "Bending Fatigue of Carburized and Shot Peened Alloy Steels", Confidential Advanced Steel Processing and Products Research Center Report, Colorado School of Mines, December, 1996.